

Available online at www.sciencedirect.com

ScienceDirect

www.elsevier.com/locate/jes

JES
 JOURNAL OF
 ENVIRONMENTAL
 SCIENCES
www.jesc.ac.cn

Brominated dioxins and furans in a cement kiln co-processing municipal solid waste

Lili Yang^{1,2}, Yuyang Zhao^{1,2}, Miwei Shi³, Minghui Zheng^{1,2}, Yang Xu^{1,2}, Cui Li^{1,2}, Yuanping Yang^{1,2}, Linjun Qin^{1,2}, Guorui Liu^{1,2,*}

1. State Key Laboratory of Environmental Chemistry and Ecotoxicology, Research Center for Eco-Environmental Sciences, Chinese Academy of Sciences, Beijing 100085, China

2. University of Chinese Academy of Sciences, Beijing 100049, China

3. Hebei Engineering Research Center for Geographic Information Application, Institute of Geographical Sciences, Hebei Academy of Sciences, Shijiazhuang 050051, China

ARTICLE INFO

Article history:

Received 20 August 2018

Revised 14 December 2018

Accepted 17 December 2018

Available online 27 December 2018

Keywords:

Polybrominated dibenzo-*p*-dioxin and dibenzofuran (PBDD/F)

Cement kiln

Municipal solid waste

Dioxin

Formation mechanism

ABSTRACT

A field study and theoretical calculations were performed to clarify the levels, profiles, and distributions of polybrominated dibenzo-*p*-dioxins and dibenzofurans (PBDD/Fs) in a cement kiln co-processing solid waste, with a focus on the PBDF formation mechanism. The raw materials contributed greatly to input of PBDD/Fs into the cement kiln. The PBDD/F concentrations in the raw materials were much higher than those in particle samples from different process stages in the cement kiln. The PBDD/F concentrations in the clinkers were 1.40% of the concentrations in the raw materials, which indicated that the high destruction efficiencies for PBDD/Fs by cement kiln. PBDD/F distribution patterns in particle samples collected from different process stages indicated the cement kiln backend was a major site for PBDD/F formation. PBDFs with high levels of halogenation, such as heptabrominated furans (HpBDF), were the dominant contributors to the total PBDD/F concentrations and accounted for 42%–73% of the total PBDD/F concentrations in the particle samples. Our results showed that co-processing of municipal solid waste in a cement kiln may influence the congener profile of PBDD/Fs, especially for the higher halogenated PBDD fraction. In addition, there were significant correlations between the decabromodiphenyl ether and heptabrominated furan concentrations, which is an indicator of transformation from polybrominated diphenyl ethers to PBDD/Fs. Theoretical calculations were performed and demonstrated that elimination of HBr and Br₂ from polybrominated diphenyl ethers were the dominant formation pathways for PBDD/Fs. These pathways differed from that for polychlorinated dibenzo-*p*-dioxins and dibenzofurans (PCDD/Fs).

© 2018 The Research Center for Eco-Environmental Sciences, Chinese Academy of Sciences.

Published by Elsevier B.V.

Introduction

Persistent organic pollutants (POPs), especially polychlorinated dibenzo-*p*-dioxins and dibenzofurans (PCDD/Fs), are of particular concern because of their persistence,

bioaccumulation, and toxicity in biological systems (Gao et al., 2011; Gioia et al., 2011). The physicochemical properties and toxicities of polybrominated dibenzo-*p*-dioxins and dibenzofurans (PBDD/Fs) are similar to those of the PCDD/Fs because they are structural analogs (Du et al., 2010). Some

* Corresponding author. E-mail: grliu@rcees.ac.cn. (G. Liu).

lower brominated dioxins reportedly have higher octanol-water partition coefficients (K_{ow}) than PCDD/Fs with the same level of halogenation, which makes them more lipophilic and more toxic than the corresponding PCDD/Fs (Berchtold, 1987). The toxic equivalency factors of 2,3,7,8-tetrabrominated dioxins in rainbow trout are 1.14–2.54 times those of 2,3,7,8-tetrachlorinated dioxins (Hornung et al., 1996). The levels of PBDD/Fs in the environment and biota have increased in recent years (Choi et al., 2003; Li et al., 2008). Unintentional formation and release of PBDD/Fs from industrial activities are important sources of PBDD/Fs in the environment (Weber and Kuch, 2003; Gullett et al., 2010; Wang et al., 2010, 2015, 2016). Therefore, to reduce the environmental burden and health risks of PBDD/Fs, it is important to control the release of PBDD/Fs from various industrial activities.

Cement kiln co-processing is a promising approach for energy recovery and disposal of solid waste. However, co-processing of solid waste could increase emission of toxic and bioaccumulative POPs (Liu et al., 2015a; Pavlík et al., 2016). According to statistical data from 2012, 58% of global cement production occurs in China (Song et al., 2016). The number of cement kilns co-processing solid waste in China is increasing, and the release of POPs during co-processing of solid waste in cement kilns should be evaluated. Cement kiln co-processing of waste has been identified as an important source of PCDD/Fs in the environment (Liu et al., 2015a, 2016a, 2016b). The levels and profiles of PCDD/Fs and dioxin-like compounds have been studied for cement kilns co-processing solid waste (Conesa et al., 2011), sewage sludge (Rovira et al., 2011), incinerator fly ash (Liu et al., 2015a) and contaminated soil (Yang et al., 2012). Potential major sites in the process for PCDD/F formation have been identified by comparison of the PCDD/F levels at different sites within the cement kiln system (Zhao et al., 2017). Results have shown that tetra- to hexachlorinated dibenzofurans at the kiln backend are dominant contributors to PCDD/F levels, perhaps because of the low content of copper and alkaline conditions in the cement kiln (Zhao et al., 2017).

However, the levels, profiles and distributions of PBDD/Fs from cement kiln co-processing of municipal solid waste (MSW) have not been reported. During cement kiln operation, chlorination should be the main formation mechanism for PCDFs (Li et al., 2007; Zhao et al., 2017). However, polybrominated diphenyl ethers (PBDEs) are a dominant precursor for PBDD/Fs (Weber and Kuch, 2003). Solid waste co-processed in a cement kiln might contain high concentrations of PBDEs (Ni et al., 2016), which could act as a precursor for PBDD/Fs in the cement kiln. Therefore, it is meaningful to clarify the levels, profiles and distributions of PBDD/Fs at different points in the process for cement kiln co-processing of solid waste. Because PBDD/Fs have high molecular weights and are more easily concentrated in the fly ash than in the stack gas, their levels and profiles in fly ash can be representative of the actual formation levels and patterns during thermal processes. In addition, air pollution control devices are normally installed in industrial plants to remove contaminants from stack gas before emission to the atmosphere. Therefore, most of PBDD/Fs produced are transferred into solid residues, including fly ash, by air pollution control devices. Consequently, solid residues from cement kilns have

been investigated (Liu et al., 2015b). This knowledge could be used to improve co-processing technology for toxic waste treatment and for synchronized control of brominated POPs and their chlorinated analogs.

In this study, we conducted a field study on a cement kiln co-processing MSW. Particle samples from different sites in the cement kiln were collected and analyzed by isotope dilution high resolution gas chromatography combined with high resolution mass spectrometry. PBDD/F levels in particle samples collected from different sites were compared. The results could be helpful for identifying dominant sites for PBDD/F formation. The distributions of PBDD/Fs and PCDD/Fs were also studied and compared, and might provide important information for possible synchronized control of PBDD/Fs and PCDD/Fs.

1. Materials and methods

1.1. Cement kiln and sample collection

The cement kiln investigated in this study was a rotary kiln with a five-stage cyclone preheater for the raw feed, and a suspension preheater (SP) boiler for waste heat power generation. The rotary kiln used for clinker formation was operated at a temperature of around 1300°C. Fabric bag fiber filters were used as air pollution control devices. The cement production capacity of the investigated cement kiln was 3200 tons per day. The composition of the raw meal was 87% lime stone, 7% sewage sludge, and 1.5% clay and some other materials. The raw material was added to the cyclone preheater and passed through the precalciner. The combustible MSW was pyrolyzed in a gasification furnace and the resultant gas was passed into the cement kiln precalciner as a supplementary fuel (Jin et al., 2016). The mass of MSW co-processed in the cement kiln was 72 tons per day. The waste contained filtered plastics (17%–35%), paper, kitchen waste, textiles, and wood. Coal (430.5 tons per day) was added to the precalciner as the main fuel. A diagram of the investigated cement kiln is published in our previous research (Jin et al., 2016, 2017).

Particle samples were collected from different stages of the cement kiln. The stages were the cyclone preheater outlet, SP boiler and humidifier tower, clinker, raw meal, and bag filters at the back end and head of the kiln (Fig. 1). Particle samples CK1–CK8 were collected from a blank run without co-processing of MSW in the cement kiln, and were analyzed for PBDD/Fs to provide reference data. Samples CK8–CK15 were collected from the cement kiln during co-processing of MSW.

1.2. PBDD/F analysis

We investigated ten 2,3,7,8-brominated PBDD/F congeners, and could not include more congeners in this study because the corresponding $^{13}\text{C}_{12}$ -labeled PBDD/F standards were not available. The sample pretreatment method is detailed elsewhere (Wang et al., 2015; Zhao et al., 2017). First, the particle samples were spiked with $^{13}\text{C}_{12}$ -labeled PBDD/F internal standards (EDF-5408; Cambridge Isotope Laboratories, Andover, MA, USA), then digested in 1 mol/L HCl, rinsed

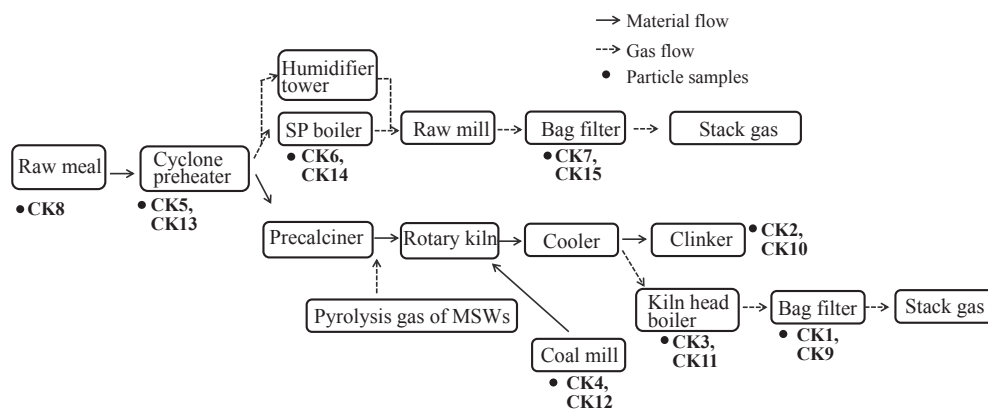


Fig. 1 – A schematic of the operation processes in cement kilns and the sampling points for particle samples. SP boiler: suspension preheater boiler. CK1-CK8 were the particle samples collected from a blank run without co-processing of MSW; CK9-CK15 were particle samples collected from the cement kiln during co-processing of MSW.

with distilled water, and freeze-dried. The samples were Soxhlet extracted with toluene for 24 hr. Each extract was then concentrated by a rotary evaporator and purified using the following two columns in sequence: a multilayer silica gel column and a basic alumina column. The multilayer silica gel column was packed with 44% (mass fraction) sulfuric acid silica gel and 33% (mass fraction) sodium hydroxide silica gel. The PBDD/F fraction was separated from the interfering compounds using a silica gel column containing 1.5 g of the mixture of activated carbon (80–100 meshes, Sigma-Aldrich, USA) and the dispersing agent (Celite 545, Sigma-Aldrich, USA) with mass ratio of 18:82. The fraction was then concentrated to 20 μL on a rotary evaporator and under a gentle stream of N_2 . Then, $^{13}\text{C}_{12}$ -labeled PBDD/F injection standards (EDF-5409; Cambridge Isotope Laboratories, England) were added to calculate the recovery.

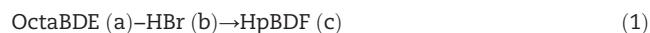
Identification and quantification of PBDD/F congeners were performed by isotope dilution high-resolution gas chromatography combined with high-resolution mass spectrometry (Trace GC Ultra coupled to a DFS mass spectrometer, Thermo Fisher Scientific, Waltham, USA) with electron ionization. Selected ion monitoring mode was used for data acquisition and the high-resolution mass spectrometer was operated at a resolution of approximately 10,000. PBDD/F congeners were separated on DB-5 MS capillary column (15 m \times 0.25 mm, 0.1 μm , Agilent, Palo Alto, USA). The electron emission energy was set to 45 eV and the source temperature was 280°C.

The recovery range for $^{13}\text{C}_{12}$ -labeled PBDD/F internal standards was 30% to 120%, and met the requirements for PBDD/F analysis by the isotope dilution method. One laboratory blank experiment was carried out for each batch of samples to confirm there were no obvious interferences for sample quantification.

1.3. Density functional theory calculation

The Gaussian 09 suite of programs was used for density functional theory calculations (Zhao et al., 2017). As a reasonable compromise between computational time and

accuracy, the MPWB1K method and a standard 6-31 + G(d,p) basis set were chosen for optimization of the geometries of the congeners (Zhao and Truhlar, 2004; Liu et al., 2016a). The relative energy of formation could be calculated from the Gibbs free energies (G), as shown in the equations below with octaBDE as an example (Eqs. (1) and (2)).



$$\Delta G = G_{(c)} - G_{(a)} + G_{(b)} \quad (2)$$

where, OctaBDE (a) is octabromodiphenyl ethers; HBr (b) is hydrogen bromide; HpBDF (c) is heptabrominated furans; ΔG (kcal/mol) is Gibbs free energy; $G_{(c)}$ (kcal/mol), $G_{(a)}$ (kcal/mol) and $G_{(b)}$ (kcal/mol) is the Gibbs free energy of HpBDF, OctaBDE and HBr, respectively.

2. Results and discussion

2.1. PBDD/F concentrations in particle samples from the cement kiln

The PBDD/F levels in particle samples collected from different process stages are shown in Fig. 2a. The highest PBDD/F concentration (1.3 ng/g) was detected in the raw material (CK8), which indicates that the raw materials have a large contribution to the input of PBDD/Fs. The PBDD/F concentrations in the particle samples collected from the different stages were much lower than that in the raw material. Relatively high PBDD/F concentrations occurred in particle samples collected from the coal mill (CK4, 0.22 ng/g), bag filters at the backend of the cement kiln (CK7, 0.19 ng/g), and the SP boiler (CK6, 0.15 ng/g), when MSWs were not co-processed. All these stages use relatively low temperatures, which are appropriate for the formation of PBDD/Fs. The PBDD/F yield as a function of the incineration temperature showed that the highest PBDD/F concentrations occurred at 600°C, and the PBDD/F concentrations decreased as the temperature increased (Dumler et al., 1990). The PBDD/F concentration in the clinkers was 0.018 ng/g, which was

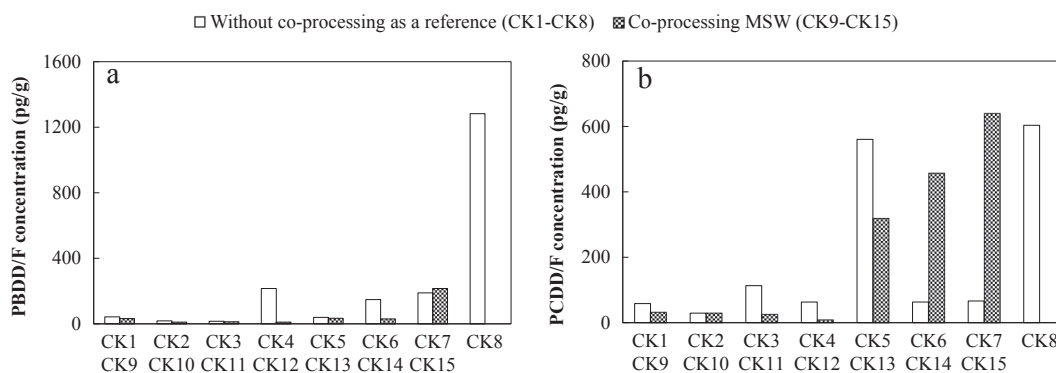


Fig. 2 – (a) Polybrominated dibenzo-*p*-dioxins and dibenzofuran (PBDD/F) and (b) polychlorinated dibenzo-*p*-dioxins and dibenzofuran (PCDD/F) levels in particle samples from a cement kiln co-processing MSW and a reference sampling campaign (no MSW co-processing). The PCDD/F data were from our previous study (Zhao et al., 2017).

about 1.40% of PBDD/F concentration in the raw materials. The fact the PBDD/F concentrations in emissions from the cement kiln process were much lower than those in the raw materials demonstrates high destruction efficiencies for the stable organic compounds. In addition, the PBDD/F concentration range in fly ash samples from the investigated cement kiln was 0.032–0.22 ng/g, and this concentration range was lower than that for fly ash samples from iron ore sintering plants (0.10–1.65 ng/g) (Wang et al., 2018). In the present study, the PBDD/F concentrations in particle samples collected from the coal mill (CK12), bag filters at the backend of the cement kiln (CK15), and SP boiler (CK14) were 0.011, 0.22, and 0.030 ng/g, respectively. The co-processing of MSW would not increase the emissions of PBDD/Fs, and there were no obvious differences in the PBDD/F concentrations between samples collected at the same processing site during the blank runs (CK1, CK2, CK3) and the runs with co-processing of MSWs (CK9, CK10, CK11). The particle samples labeled as CK9, CK10 and CK11 were collected during the processes after that the MSW pyrolysis gas was added. This confirmed the strong destruction ability of the cement kiln for PBDD/Fs. The high temperature and alkaline environment of the cement kiln contribute to its high destruction efficiency, and this knowledge could be used for the control of POPs formed in other industrial processes.

The PCDD/F concentrations in particle samples collected from different process stages are shown in Fig. 2b. The PCDD/F determination method is detailed in our previous study (Zhao et al., 2017). With co-processing of MSW in the cement kiln, the concentrations of seventeen 2,3,7,8-PCDD/Fs in particle samples collected from preheater outlet, SP boiler, and bag filters were 0.32, 0.46 and 0.64 ng/g, respectively. In the reference sampling campaign, the PCDD/F concentrations in particle samples collected from the preheater outlet, SP boiler, and bag filters at the backend of the cement kiln were 0.56, 0.063 and 0.066 ng/g, respectively (Zhao et al., 2017). These results show that the PCDD/F concentrations in the SP boiler and bag filters increased when MSWs were co-processed. By contrast, no obvious differences in the PBDD/F concentrations were observed in the same process stages. Therefore, compared with PBDD/Fs, the PCDD/F concentrations are substantially influenced by the co-processing of

MSW in the cement kiln. This might be a result of the higher molecular weights of the PBDD/Fs compared with the PCDD/Fs, which could result in low stability at high temperatures in cement kilns.

2.2. PBDD/F congener profiles in particle samples from the cement kiln

Congener profiles were constructed for the PBDD/Fs in particle samples from the cement kiln during co-processing MSW and in the reference sampling campaign without MSW co-processing (Fig. 3). PBDF was dominant in all of the samples. In most cases, the PBDFs yield was considerably higher than that of PBDDs (Dumler et al., 1990; Duan et al., 2011; Zhang et al., 2016). This may be explained by the loss of an ortho-Br or -H atom from PBDE, a typical precursor of PBDD/Fs, followed by ring closure as the most accessible pathway. Therefore, compared with PBDDs formed by oxidation and ring closure, which is a complex exothermic mechanism (Zhang et al., 2016), PBDFs can form more easily during thermal processes. Higher halogenated PBDFs, such as HpBDF, were the dominant contributors to the total PBDD/F concentrations, accounting for 42%–73% of the total PBDD/Fs in different particle samples, followed by hexabrominated furan (HxBDF) and HpBDD. The fraction of HpBDD increased in the particle samples collected from the clinker formation process, boiler at the kiln head, and the coal mill, indicating that HpBDD was formed mainly after that the MSW pyrolysis gas was added to the cement kiln precalciner. Meanwhile, the fractions of HpBDF and HxBDF decreased. Metals and metal oxides in the pyrolysis gas may contribute to this phenomenon (Xia et al., 2017; Zhang et al., 2016). In the presence of catalytic metals such as iron, zinc, tin, copper and metal oxides, the distribution pattern changes towards higher halogenated PBDDs (Lenoir et al., 1994). Therefore, co-processing of MSW in cement kilns may influence the congener profile of PBDD/Fs, and increase the higher halogenated PBDD fraction. Consequently, the destruction and formation mechanisms of PBDD/Fs in the cement kiln need to be further studied in detail, and could be enlightening for developing emission reduction techniques for persistent organic pollutants from the other industrial sources.

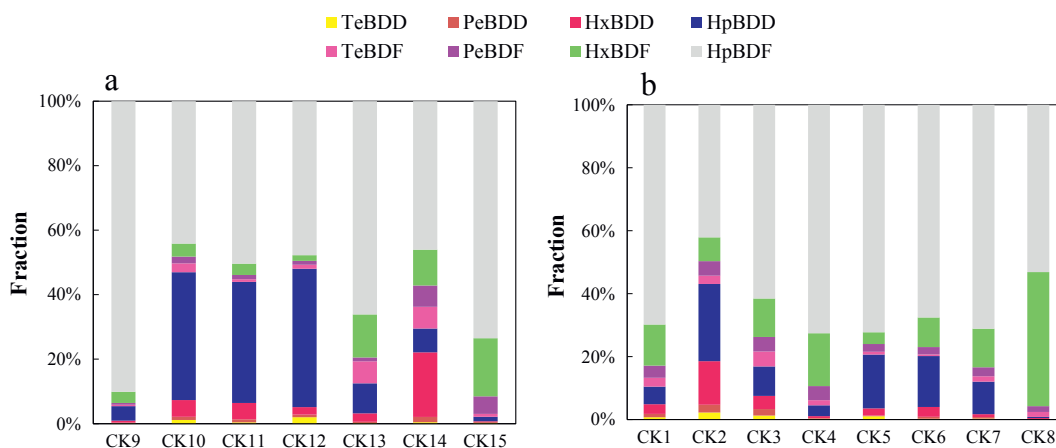


Fig. 3 – PBDD/F profiles in particulate samples from (a) a cement kiln co-processing MSW and (b) a blank run without MSW co-processing.

The congener profiles of the PCDD/Fs and PBDD/Fs from the investigated cement kiln were compared. Formation of tetra- to hexachlorinated dibenzofurans dominated at the main formation sites in the cement kiln during co-processing of MSW, and accounted for 50%–80% of the total PCDD/F mass concentrations (Zhao et al., 2017). The 2,3,7,8-PCDF is supposedly formed via successive chlorination of lower chlorinated dibenzofurans (Zhao et al., 2017). Therefore, the dominant PCDD/F congeners were quite different from those of the PBDD/Fs in particle samples from the same cement kiln. Reportedly, brominated flame retardants (BFRs) can form PBDD/Fs through a precursor pathway, even under only mild thermal stress (Zhang et al., 2016). Consequently, even though the PBDD/Fs and PCDD/Fs have quite similar structures, the congener fraction showed that the formation mechanism of PBDD/Fs was different from that of the PCDD/Fs. This possibly occurred because the BFRs also act as specific precursors to form additional PBDD/Fs.

2.3. Possible formation mechanism of PBDD/Fs

PBDEs are an important precursor of PBDD/Fs during thermochemical reactions. Industrial PBDE products reportedly mainly contain penta-, octa-, and decabromodiphenyl ether (BDE-209), with BDE-209 accounting for about 83% of the total consumption of industrial PBDEs in 2001 (Soderstrom et al., 2004). As a result, in sediments, atmospheric particle samples and water samples, especially ones collected near factories and electronic waste disposal sites, BDE-209 is present at the highest concentration among all the congeners, even though it was banned by the European Union in 2008 (Soderstrom et al., 2004). Therefore, in this study, the relationship between the concentrations of BDE-209 and 1,2,3,4,6,7,8-HpBDF was investigated. The correlation between BDE-209 and 1,2,3,4,6,7,8-HpBDF concentrations in the particle samples collected from different operation stages was significant (Fig. 4, correlation coefficient of 0.82), which was an indicator of potential transformation of BDE-209 to PBDD/Fs. The results were in accordance with those from previous studies, which

reported that 1,2,3,4,6,7,8-HpBDF was the prevailing congener in some commercial decabromodiphenyl ether mixtures (Ren et al., 2011).

It has been shown that the dominant formation mechanism of PBDD/Fs is quite different from that of PCDD/Fs. To further validate the formation mechanism of PBDD/Fs, the formation energies of the HpBDFs were calculated according to the isodesmic reactions. Debromination from octabrominated furans to HpBDF was expected to be an energetically feasible reaction (Fig. 5). The debromination reaction can easily occur because of the high molecular weights and low stabilities of higher brominated PBDFs. In addition, HpBDFs can easily form through the energetically favorable intramolecular elimination of HBr or Br₂ from octabromodiphenyl ether (Gibbs free energy of 2.8 kcal/mol) or nonabromodiphenyl ether (Gibbs free energy of 18.5 kcal/

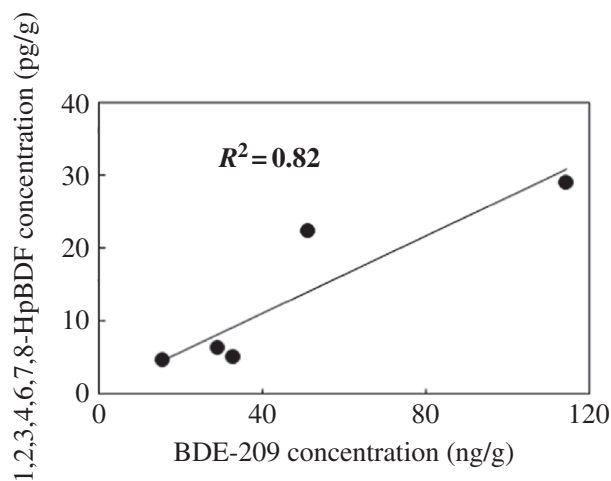


Fig. 4 – Plot of the concentrations of 1,2,3,4,6,7,8-heptabrominated furans (HpBDFs) against BDE-209 from particle samples collected from cement kiln co-processing municipal solid waste.

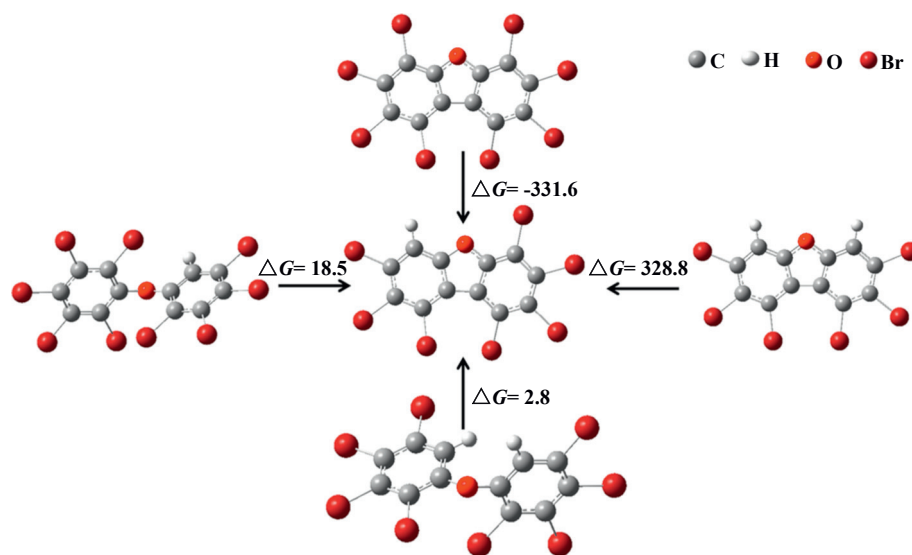


Fig. 5 – Gibbs free energies (ΔG , kcal/mol) of isodesmic reactions for the formation of heptabrominated furans (HpBDFs).

mol). Hexabrominated furans are energetically unfavorable with much a higher Gibbs free energy (328.8 kcal/mol). The results further validate the different formation mechanisms of PBDFs and PCDFs, and prove PCDFs are formed mainly by chlorination of lower chlorinated PCDFs during cement kiln processing (Zhao et al., 2017). Therefore, according to the experimental and calculation results, in addition to de novo formation and precursor dimerization (Zhang et al., 2016), PBDD/Fs are largely formed through elimination of HBr and Br₂ from PBDEs, which is quite different to the formation pathway for PCDD/Fs.

3. Conclusions

This study investigated the levels, profiles and distributions of PBDD/Fs from a cement kiln co-processing solid waste. The cement kiln had high destruction efficiencies for PBDD/Fs as the concentrations in raw materials were much higher than those in particles from different stages. The distribution pattern in particle samples showed the backend of the cement kiln was a major formation site. Higher halogenated PBDFs were the dominant contributor to the total PBDD/F concentrations, and HpBDF accounted for 42%–73% of the total concentration. Our experimental and theoretical results show that PBDEs are the dominant precursor of PBDFs, and can be transformed into PBDFs through elimination of HBr and Br₂. The dominant formation mechanism of PBDFs is different from that of PCDD/Fs, which are formed by chlorination of lower chlorinated PCDD/Fs. These results increase our understanding of pollutant emissions from cement kilns, and could be used for synchronized control of PBDD/Fs and PCDD/Fs.

Conflict of interest

There is no conflict of interest.

Acknowledgments

This work was supported by the National Natural Science Foundation of China (No. 21777172), the Collaborative Project supported by Chinese Academy of Sciences and Hebei Academy of Sciences (No. 181602), and the Youth Innovation Promotion Association of the Chinese Academy of Sciences (No. 2016038).

REFERENCES

- Berchtold, F.R., 1987. Prediction of vapor pressures, boiling points and enthalpies of fusion for twenty-nine halogenated dibenzo-*p*-dioxins. *Thermochim. Acta* 117–122.
- Choi, J.W., Fujimaki, S., Kitamura, K., Hashimoto, S., Ito, H., Suzuki, N., et al., 2003. Polybrominated dibenzo-*p*-dioxins, dibenzofurans, and diphenyl ethers in Japanese human adipose tissue. *Environ. Sci. Technol.* 37, 817–821.
- Conesa, J.A., Rey, L., Egea, S., Rey, M.D., 2011. Pollutant formation and emissions from cement kiln stack using a solid recovered fuel from municipal solid waste. *Environ. Sci. Technol.* 45, 5878–5884.
- Song, D., Yang, J., Chen, B., Hayat, T., Alsaedi, A., 2016. Life-cycle environmental impact analysis of a typical cement production chain. *Appl. Energy* 164, 916–923.
- Du, B., Zheng, M.H., Tian, H.H., Liu, A.M., Huang, Y.R., Li, L.L., et al., 2010. Occurrence and characteristics of polybrominated dibenzo-*p*-dioxins and dibenzofurans in stack gas emissions from industrial thermal processes. *Chemosphere* 80, 1227–1233.
- Duan, H., Li, J., Liu, Y., Yamazaki, N., Jiang, W., 2011. Characterization and inventory of PCDD/Fs and PBDD/Fs emissions from the incineration of waste printed circuit board. *Environ. Sci. Technol.* 45, 6322–6328.
- Dumler, R., Lenoir, D., Thoma, H., Hutzinger, O., 1990. Thermal formation of polybrominated dibenzofurans and dioxins from decabromodiphenyl ether flame-retardant - influence of antimony(iii) oxide and the polymer matrix. *Chemosphere* 20, 1867–1873.

- Gao, L.R., Zheng, M.H., Zhang, B., Liu, W.B., Xiao, K., Su, G.J., et al., 2011. Poly chlorinated dibenzo-*p*-dioxins and dibenzofurans in different tissues of the cormorants (*Phalacrocorax carbo*) from Dongting Lake, China. *J. Environ. Sci.* 23, 1709–1713.
- Gioia, R., Eckhardt, S., Breivik, K., Jaward, F.M., Prieto, A., Nizzetto, L., et al., 2011. Evidence for major emissions of PCBs in the west African region. *Environ. Sci. Technol.* 45, 1349–1355.
- Gullett, B.K., Wyrzykowska, B., Grandesso, E., Touati, A., Tabor, D. G., Ochoa, G.S., 2010. PCDD/F, PBDD/F, and PBDE emissions from open burning of a residential waste dump. *Environ. Sci. Technol.* 44, 394–399.
- Hornung, M.W., Zabel, E.W., Peterson, R.E., 1996. Toxic equivalency factors of polybrominated dibenzo-*p*-dioxin, dibenzofuran, biphenyl, and polyhalogenated diphenyl ether congeners based on rainbow trout early life stage mortality. *Toxicol. Appl. Pharmacol.* 140, 227–234.
- Jin, R., Zhan, J.Y., Liu, G.R., Zhao, Y.Y., Zheng, M.H., 2016. Variations and factors that influence the formation of polychlorinated naphthalenes in cement kilns co-processing solid waste. *J. Hazard. Mater.* 315, 117–125.
- Jin, R., Zhan, J.Y., Liu, G.R., Zhao, Y.Y., Zheng, M.H., Yang, L.L., et al., 2017. Profiles of polychlorinated biphenyls (PCBs) in cement kilns co-processing solid waste. *Chemosphere* 174, 165–172.
- Lenoir, D., Zier, B., Bieniek, D., Kettrup, A., 1994. The influence of water and metals on PBDD/F concentration in incineration of decabromodiphenyl ether in polymeric matrices. *Chemosphere* 28, 1921–1928.
- Li, X.D., Zhang, J., Yan, J.H., Cen, K.F., Ryan, S.P., Cullett, B.K., et al., 2007. Experimental and modeling study of de novo formation of PCDD/PCDF on MSW fly ash. *J. Environ. Sci.* 19, 117–122.
- Li, H.R., Feng, H.L., Sheng, G.Y., Lu, S.L., Fu, J.M., Peng, P.A., et al., 2008. The PCDD/F and PBDD/F pollution in the ambient atmosphere of Shanghai, China. *Chemosphere* 70, 576–583.
- Liu, G.R., Zhan, J.Y., Zheng, M.H., Li, L., Li, C., Jiang, X.X., et al., 2015a. Field pilot study on emissions, formations and distributions of PCDD/Fs from cement kiln co-processing fly ash from municipal solid waste incinerations. *J. Hazard. Mater.* 299, 471–478.
- Liu, G.R., Jiang, X.X., Wang, M., Dong, S.J., Zheng, M.H., 2015b. Comparison of PCDD/F levels and profiles in fly ash samples from multiple industrial thermal sources. *Chemosphere* 133, 68–74.
- Liu, G.R., Zhan, J.Y., Zhao, Y.Y., Li, L., Jiang, X.X., Fu, J.J., et al., 2016a. Distributions, profiles and formation mechanisms of polychlorinated naphthalenes in cement kilns co-processing municipal waste incinerator fly ash. *Chemosphere* 155, 348–357.
- Liu, G.R., Yang, L.L., Zhan, J.Y., Zheng, M.H., Li, L., Jin, R., et al., 2016b. Concentrations and patterns of polychlorinated biphenyls at different process stages of cement kilns co-processing waste incinerator fly ash. *Waste Manag.* 58C, 280–286.
- Ni, H.G., Lu, S.Y., Mo, T., Zeng, H., 2016. Brominated flame retardant emissions from the open burning of five plastic wastes and implications for environmental exposure in China. *Environ. Pollut.* 214, 70–76.
- Pavlík, Z., Fořt, J., Záleská, M., Pavlíková, M., Trnák, A., Medved, I., et al., 2016. Energy-efficient thermal treatment of sewage sludge for its application in blended cements. *J. Clean. Prod.* 112, 409–419.
- Ren, M., Peng, P., Cai, Y., Chen, D., Zhou, L., Chen, P., et al., 2011. PBDD/F impurities in some commercial deca-BDE. *Environ. Pollut.* 159 (5), 1375–1380.
- Rovira, J., Mari, M., Nadal, M., Schuhmacher, M., Domingo, J.L., 2011. Use of sewage sludge as secondary fuel in a cement plant: human health risks. *Environ. Int.* 37, 105–111.
- Soderstrom, G., Sellstrom, U., Wit, C.A.D., Tysklind, M., 2004. Photolytic debromination of decabromodiphenyl ether (BDE 209). *Environ. Sci. Technol.* 38, 127–132.
- Wang, L.C., His, H.C., Wang, Y.F., Lin, S.L., Chang-Chien, G.P., 2010. Distribution of polybrominated diphenyl ethers (PBDEs) and polybrominated dibenzo-*p*-dioxins and dibenzofurans (PBDD/Fs) in municipal solid waste incinerators. *Environ. Pollut.* 158, 1595–1602.
- Wang, M., Liu, G.R., Jiang, X.X., Liu, W.B., Li, L., Li, S.M., et al., 2015. Brominated dioxin and furan stack gas emissions during different stages of the secondary copper smelting process. *Atmos. Pollut. Res.* 6, 464–468.
- Wang, M., Liu, G.R., Jiang, X.X., Zheng, M.H., Yang, L.L., Zhao, Y.Y., et al., 2016. Thermochemical formation of polybrominated dibenzo-*p*-dioxins and dibenzofurans mediated by secondary copper smelter fly ash, and implications for emission reduction. *Environ. Sci. Technol.* 50, 7470–7479.
- Wang, M., Li, Q.Q., Liu, W.B., 2018. Effects of desulfurization processes on polybrominated dibenzo-*p*-dioxin and dibenzofuran emissions from iron ore sintering. *Environ. Sci. Technol.* 52, 5764–5770.
- Weber, R., Kuch, B., 2003. Relevance of bfrs and thermal conditions on the formation pathways of brominated and brominated-chlorinated dibenzodioxins and dibenzofurans. *Environ. Int.* 29, 699–710.
- Xia, Y., He, P.J., Shao, L.M., Zhang, H., 2017. Metal distribution characteristic of mswi bottom ash in view of metal recovery. *J. Environ. Sci.* 52, 178–189.
- Yang, Y., Huang, Q., Tang, Z., Wang, Q., Zhu, X., Liu, W., 2012. Deca-brominated diphenyl ether destruction and PBDD/F and PCDD/F emissions from coprocessing deca-BDE mixture-contaminated soils in cement kilns. *Environ. Sci. Technol.* 46, 13409–13416.
- Zhang, M., Buekens, A., Li, X., 2016. Brominated flame retardants and the formation of dioxins and furans in fires and combustion. *J. Hazard. Mater.* 304, 26–39.
- Zhao, Y., Truhlar, D.G., 2004. Hybrid meta density functional theory methods for thermochemistry, thermochemical kinetics, and noncovalent interactions: the MPW1B95 and MPWB1K models and comparative assessments for hydrogen bonding and van der waals interactions. *J. Phys. Chem. A* 108, 6908–6918.
- Zhao, Y.Y., Zhan, J.Y., Liu, G.R., Ren, Z.Y., Zheng, M.H., Jin, R., et al., 2017. Field study and theoretical evidence for the profiles and underlying mechanisms of PCDD/F formation in cement kilns co-incinerating municipal solid waste and sewage sludge. *Waste Manag.* 61, 337–344.